Journal of Applied Polymer Science

Poly[6-(2,6-bis(1′-methylbenzimidazolyl)pyridin-4-yloxy)hexyl acrylate] (PBIP) and its terbium (III) complex (PBIP-Tb^{3+}): Homopolymerization, optical, and magnetic performance

Dizheng Liu, Weilin Sun, Rong Ren, Yanhua Wang, Zhiquan Shen

MOE Key Laboratory of Macromolecular Synthesis and Functionalization, Department of Polymer Science and Engineering, Zhejiang University, Hangzhou, 310027, People's Republic of China

Correspondence to: W. Sun (E-mail: opl_sunwl@zju.edu.cn)

ABSTRACT: Poly[6-(2,6-bis(1′-methylbenzimidazolyl)pyridin-4-yloxy)hexyl acrylate] (PBIP) and its terbium complex (PBIP-Tb^{3+}) were prepared and characterized by ^{1}H NMR and FT-IR. The optical properties of PBIP-Tb^{3+} complex were characterized by UV–vis spectroscopy and fluorescence spectroscopy. Both polymer PBIP and PBIP-Tb^{3+} complex show good thermal stability. The magnetic property of PBIP-Tb^{3+} complex was measured as a function of temperature (5–300 K) at 30 kOe and as a function of an external field (−50 to 50 kOe) at 5 K. Magnetic hysteresis loop of PBIP-Tb^{3+} complex at 5 K shows typical "S" shape and PBIP-Tb^{3+} complex is soft ferromagnetic. © 2016 Wiley Periodicals, Inc. J. Appl. Polym. Sci. **2016**, *133*, 44249.

KEYWORDS: magnetism; magnetic properties; optical properties; thermal properties

Received 18 January 2016; accepted 23 July 2016
DOI: 10.1002/app.44249

INTRODUCTION

Organic magnetic materials have been explored intensively in recent decades owing to low relative density, good magnetic performance, structural variability and easy processing. They are widely used as micro-wave absorption materials,[1] high frequency devices,[2] and high density storage materials.[3,4] Among organic magnetic materials, polymeric metal complexes are mainly studied because of their simple synthesis, various ligands and diverse coordinated modes[5–9] and their magnetism comes from the long range ordering of unpaired electrons through spin-spin interactions.[10]

2,6-Bis(2-benzimidazolyl)pyridine (BIP) derivate is an important family of tridentate chelate ligands. They have strong coordinating capability and can chelate with both transition metal ions and lanthanide ions.[11–13] Their complexes display good biocompatibility,[14,15] excellent catalytic activity,[16,17] high sensitivity and selectivity to specific matter,[18–20] special optical and electrical property,[21–23] and interesting magnetism,[24–26] so they have aroused a great of interest for their potential applications. Up to now, several small molecular magnets containing BIP complexes have been reported.[26–28] However, magnetic properties of polymeric lanthanide complexes with BIP derivate as the chelating ligands have seldom been investigated.

2,6-Bis(1′-methylbenzimidazolyl)pyridine (MeBIP) is one of BIP derivate and its homopolymer poly[6-(2,6-bis(1′-methylbenzimidazolyl)pyridin-4-yloxy)hexyl acrylate] (PBIP) was rarely studied. In this article, homopolymer PBIP and its terbium complex were prepared. The structural, optical, thermal and magnetic properties were examined. The results indicate that PBIP-Tb^{3+} complex is soft ferromagnetic material with good thermal stability.

EXPERIMENTAL

Materials

Chelidamic acid and *N*-methyl-1,2-phenylenediamine dihydrochloride were purchased from TCI and used without further purification. Terbium nitrate (99.9%) was purchased from STREM. $Tb(NO_3)_3$ was purchased from TCI. 2,2′-Azobisisobutyronitrile (AIBN, AkzoNobel, 98%) was recrystallized from methanol before use. Chlorobenzene was purchased from Aldrich. Tetrahydrofuran (THF) was used after distillation in the presence of sodium. Cyanic (S-dodecyl carbonodithioic) thioanhydride (CTA) was prepared according to the report.[29] All other reagents were analytical grade and used without further purification.

Instrumentation

NMR spectra were obtained on a Varian spectrometer (400 MHz) with deuterated chloroform ($CDCl_3$) as the solvent and tetramethylsilane (TMS) as the internal standard. Fourier

Additional Supporting Information may be found in the online version of this article.

transform infrared (FT-IR) spectra were obtained on a Bruker Vector 22 FT-IR spectrometer based on KBr pellet method. Gel permeation chromatography (GPC) results were obtained by using PS as the standard and THF as the eluent. Elemental analysis for C, H, and N was obtained on an Elementar Vario CHNS-O. Tb content of PBIP-Tb^{3+} complex was measured by inductively coupling plasma mass spectrometry (ICP-MS). Electrospray ionization mass spectrum (ESI-MS) was acquired on a Thermo Finnigan LCQ DECA XP ion trap mass spectrometer, equipped with an ESI source. Ultraviolet–visible (UV–vis) absorption spectroscopy was conducted on a UV-1601 UV–vis spectrophotometer. Fluorescence spectra were obtained on a LS55 fluorescence spectrometer. The magnetic measurement was carried out by a physical properties measurement system (PPMS-9T) magnetometer (Quantum Design) as the field dependence at 5 K for magnetization (M) and as the thermal dependence between 5 and 300 K for the χT value (χ is the gram magnetic susceptibility defined by $M/(Hm)$, M being the magnetization, H the external magnetic field fixed at 30 kOe and m the mass of measured PBIP-Tb^{3+} complex). The measured amount of polymeric complex was about 100 mg.

Synthesis of Monomer 6-(2,6-bis(1′-methylbenzimidazolyl)pyridin-4-yloxy)Hexyl Acrylate (BIP)

6-MeBIP-OH (6.3 g, 13.8 mmol) (preparation in Supporting Information), triethylamine (7.7 mL, 55.2 mmol) were dissolved in 100 mL dry tetrahydrofuran (THF). The resulting solution was cooled in an ice bath followed by dropping acryloyl chloride (1.5 mL, 27.6 mmol) THF solution (10 mL). The mixture was stirred in the ice bath for 4 h and then heated to 30 °C for 24 h. After filtration, the filtrate was collected and THF was removed by reduced pressure distillation. The product obtained was dissolved in dichloromethane (CH_2Cl_2) and the solution was washed successively with saturated $NaHCO_3$, water and brine. The organic layer was collected and dried with sodium sulfate (Na_2SO_4). After filtration, the crude product was obtained by removing CH_2Cl_2, dried under high vacuum and further purified via chromatography (SiO_2; CH_2Cl_2: MeOH = 40:1).

Yield: 46%. ^{1}H NMR (400 MHz, $CDCl_3$, δ): 1.46–1.59 (m, 2H), 1.70–1.77 (m, 2H), 1.85–1.92 (m, 4H), 4.19 (t, 2H), 4.25–4.27 (m, 8H), 5.84 (dd, 1H), 6.15 (dd, 1H), 6.34 (dd, 1H), 7.35–7.41 (m, 4H, ph-H), 7.46 (d, 2H, py-H), 7.89 (d, 2H, ph-H), 7.95 (s, 2H, ph-H). ^{13}C NMR (100 MHz, $CDCl_3$, δ): 166.60(C = O), 166.34, 151.08, 150.40, 142.45, 137.18, 130.58, 128.60, 123.58, 122.85, 120.14, 111.82, 109.95, 68.49, 64.51, 32.55(CH_3), 28.80, 28.59, 25.71, 25.64. FT-IR (KBr): ν = 2944(m), 2858(m), 1724(s), 1634(w), 1591(s), 1567(s), 1444(s), 1414(m), 1388(m), 1309(m), 1200(s), 1026(s), 878(m), 862(w), 741(s) cm^{-1}. Anal. Calcd. for $C_{30}H_{31}N_5O_3$: C, 70.71; H, 6.13; N, 13.74. Found: C, 70.39; H, 6.144; N, 13.34. MS (ESI, m/z): $[M+H]^+$ calcd for $C_{30}H_{31}N_5O_3$, 510.6; found, 510.4.

RAFT Homopolyerization of the Monomer BIP

BIP (101.9 mg, 0.2 mmol), CTA (3.17 mg, 0.01 mmol), and AIBN (0.82 mg, 0.005 mmol) were added into 1 mL chlorobenzene. After three freeze–thawing cycles, the mixture was placed in a temperature-controlled oil bath at 70 °C. The mixture was stirred for 24 h before exposure to atmosphere. The resulting homopolymer was precipitated in the mixture of ethyl acetate and petroleum ether (7:1 v/v) for three times, collected by centrifugation, and dried under high vacuum to obtain a yellowish solid.

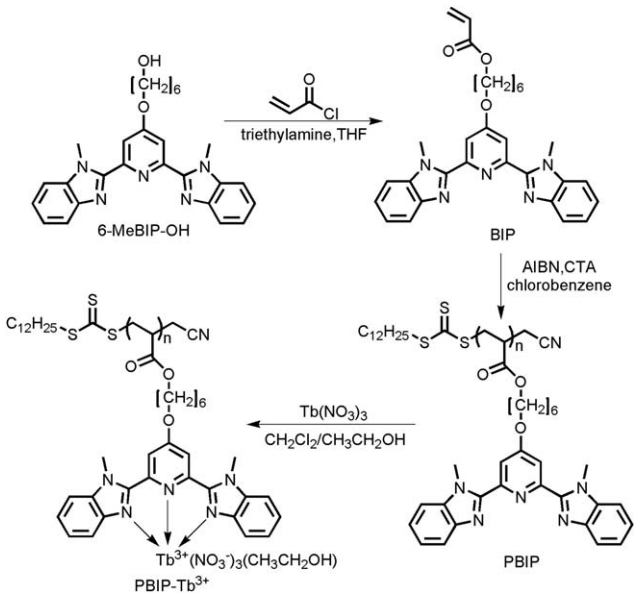

Scheme 1. Preparation of monomer (BIP), homopolymer (PBIP), and complex (PBIP-Tb^{3+}).

Conversion: 98%. ^{1}H NMR (400 MHz, $CDCl_3$, δ): 0.82 (s, 1H), 1.14–1.66 (m, 22H), 2.30 (s, 6H), 4.13 (s, 20H), 7.26 (m, 14H), 7.82 (s, 8H). FT-IR (KBr): ν = 2944(m), 2861(w), 1724(s), 1591(s), 1567(s), 1444(s), 1414(m), 1388(m), 1309(m), 1200(s), 1026(m), 878(m), 862(w), 741(s) cm^{-1}.

Preparation of PBIP-Tb^{3+} Complex

PBIP-Tb^{3+} complex was prepared as follows. 5 mL ethanol of $Tb(NO_3)_3$ (103.5 mg, 0.3 mmol) was slowly dropped into 15 mL dichloromethane (CH_2Cl_2) solution of PBIP (153.0 mg, amount of repeat unit: 0.3 mmol) under nitrogen atmosphere. The mixture was refluxed at 60 °C for 24 h. The precipitate was formed, filtrated and washed with diethyl ether to remove metal ions, dried under high vacuum to obtain a white solid.

Yield = 41%. Tb (wt %)=7.3%. FT-IR (KBr): 3436(m), 2931(m), 2856(w), 1724(m), 1604(m), 1565(m), 1490(s), 1385(s), 1310(s), 1186(m), 1143(w), 1027(m), 874(w), 815(m), 748(s) cm^{-1}.

RESULTS AND DISCUSSION

Structural Property of Monomer BIP, Homopolymer PBIP, and PBIP-Tb^{3+} Complex

Scheme 1 illustrates the preparation route of monomer BIP, homopolymer PBIP, and PBIP-Tb^{3+} complex. Figures 1 and 2 show ^{1}H NMR spectra and FT-IR spectra of BIP and PBIP, respectively. For BIP [Figure 1(a)], the peaks at 5.84, 6.15, and 6.34 ppm are attributed to hydrogens of the vinyl groups (—CH_2═CH) and the peak at 4.19 ppm belongs to hydrogens nearest to the hydroxyl (—CH_2OH). For PBIP [Figure 1(b)], the disappearance of peaks between 5.84 and 6.34 ppm confirms

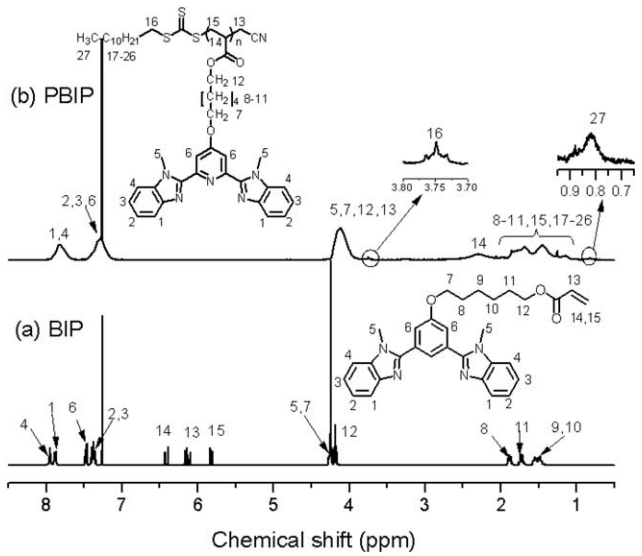

Figure 1. (a,b) ^{1}H NMR spectra of monomer BIP (a) and homopolymer PBIP (b).

the successful synthesis of PBIP.[13,30] The result of FT-IR spectra also supports the conclusion. There are two characteristic peaks at 1634 and 1724 cm^{-1} in FT-IR spectrum of BIP [Figure 2(a)], corresponding to the stretching vibration of C═C and the skeletal vibration of the C═O. But no peak is at 1634 cm^{-1} for PBIP [Figure 2(b)].

To characterize the structure of PBIP-Tb^{3+} complex, FT-IR (Figure 2) and UV–vis (Figure 3) were employed. After coordinating with Tb^{3+}, the vibration of the C═N bond of imidazole ring shifts from 1591 to 1604 cm^{-1}. This is because the energy transfers from MeBIP ligands of PBIP to Tb^{3+}.[31] Shape and intensity of all peaks change a lot, indicating that the MeBIP ligands form stable complexes with Tb^{3+}. Figure 4 illustrates UV-vis spectra of solutions of PBIP with different concentrations of $Tb(NO_3)_3$. The color gradient represents a changing concentration of $Tb(NO_3)_3$ in increments of 0.26 mmol

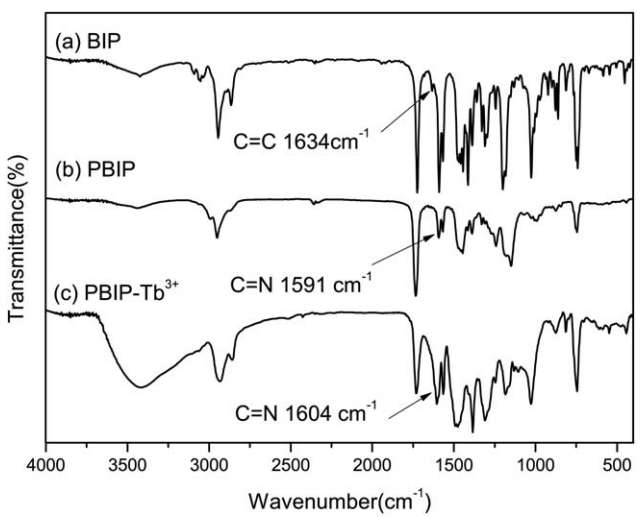

Figure 2. (a–c) FT-IR spectra of monomer BIP (a), homopolymer PBIP (b), and polymeric complex PBIP-Tb^{3+} (c).

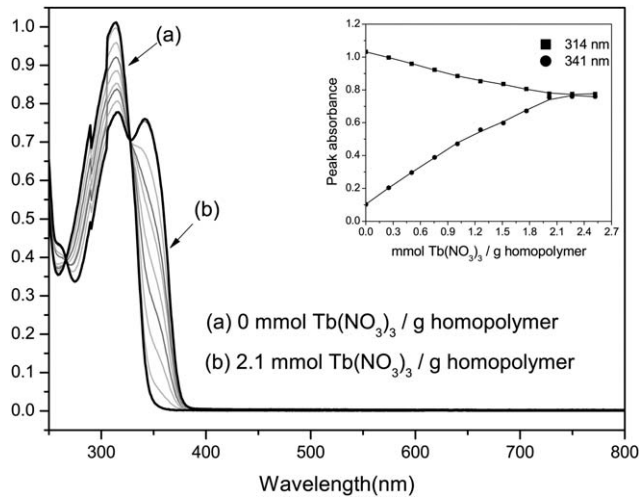

Figure 3. UV–vis spectra of solutions of PBIP with different concentrations of $Tb(NO_3)_3$. The gradient represents a changing concentration of $Tb(NO_3)_3$ in increments of 0.26 mmol $Tb(NO_3)_3$ per gram of PBIP. Inset shows the absorbance of peaks corresponding to uncomplexed ($\lambda = 314$ nm) and complexed ($\lambda = 341$ nm) MeBIP as a function of metal ion concentration.

$Tb(NO_3)_3$ per gram of PBIP. Inset shows the absorbance of peaks corresponding to uncomplexed ($\lambda = 314$ nm) and complexed ($\lambda = 341$ nm) MeBIP as a function of metal ion concentration. The peaks at 314 and 341 nm are attributed to MeBIP ligand before and after chelating with Tb^{3+}. As chelating with Tb^{3+}, the electron of MeBIP transfers to Tb^{3+} and the energy of MeBIP decreases. So the absorption peak red shifts from 314 to 341 nm. Upon addition of $Tb(NO_3)_3$, uncomplexed MeBIP decreases and complexed MeBIP increases, so the intensity of peaks at 314 and 341 nm changes and becomes saturated. As a result, the quantity of Tb^{3+} added to reach the saturation point is nearly equal to the quantity of MeBIP ligands of PBIP. Therefore, MeBIP is binding with Tb^{3+} in the ratio of 1:1.[30] This is consistent with the literature.[31] In addition, for PBIP-Tb^{3+}

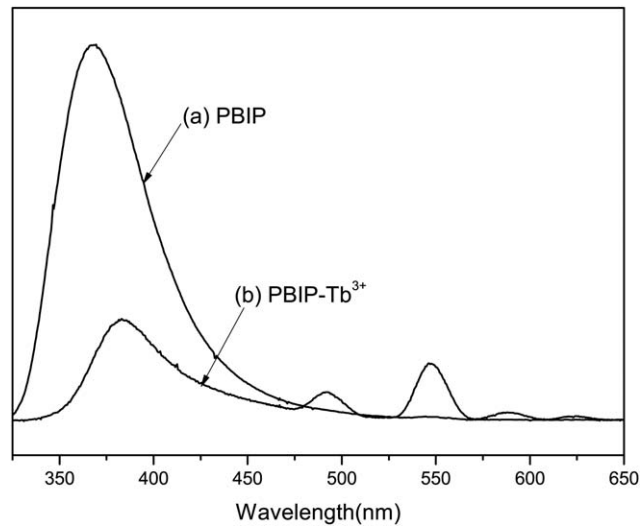

Figure 4. (a,b) Fluorescence spectra of PBIP (a) and PBIP-Tb^{3+} complex (b) excited at 314 nm.

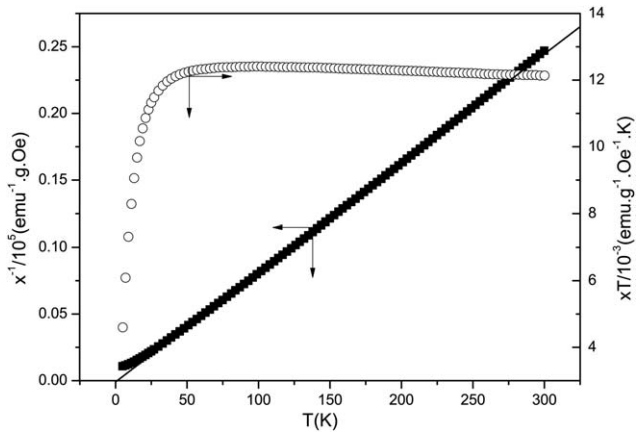

Figure 5. Temperature dependence of χT and the magnetic susceptibility (χ^{-1}) for PBIP-Tb^{3+} complex at an applied magnetic field of 30 kOe. The straight line is a fit to the Curie–Weiss law in the temperature range from 50 to 300 K.

complex, metal content is 7.3%, less than the theoretical value 17.6%. It means about 41% MeBIP ligands of PBIP form complexes with Tb^{3+}.

Optical Properties of PBIP-Tb^{3+} Complex

Materials containing Tb^{3+} offer the possibility of utilizing the interesting spectroscopic properties, so fluorescence spectra of PBIP and PBIP-Tb^{3+} complex were investigated. Figure 4(a) shows the ligand emission spectral features of PBIP under the excitation of 365 nm. For PBIP-Tb^{3+} complex [Figure 4(b)], the intense broad band at 385 nm corresponds to MeBIP excitation. After MeBIP excitation, a ligand-to-Tb energy transfer takes place from the $3\pi\pi^*$ excited state of MeBIP to the $^5D_4$ level of Tb^{3+}.[31] So four peaks appear at 491 nm ($^5D_4 \rightarrow {}^7F_6$), 547 nm ($^5D_4 \rightarrow {}^7F_5$), 588 nm ($^5D_4 \rightarrow {}^7F_4$) and 625 nm ($^5D_4 \rightarrow {}^7F_3$), indicative of the terbium metal centered emission.[32] The shift of ligand emission and the appearance of Tb^{3+} emission demonstrate that MeBIP ligand is binding to Tb^{3+}.

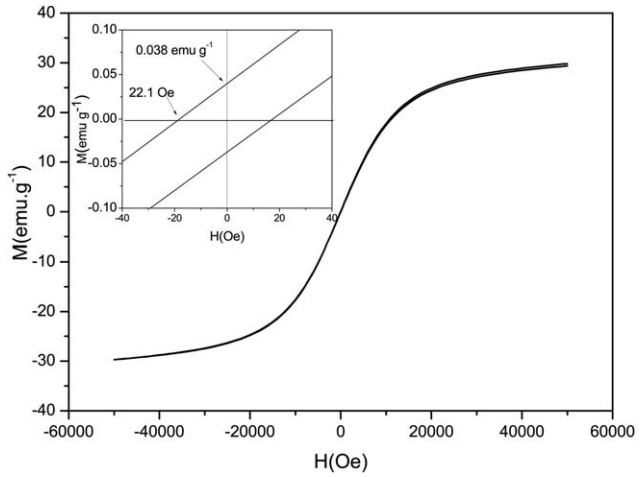

Figure 6. Magnetic hysteresis loop (M vs. H) for PBIP-Tb^{3+} complex at 5 K. Inset shows expanded view of the region from −40 to 40 Oe.

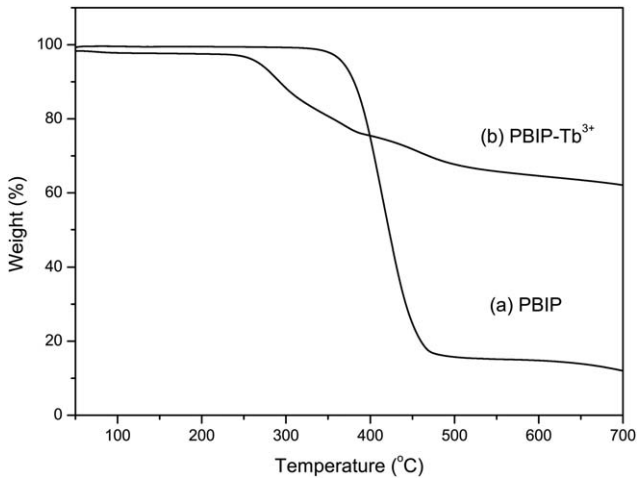

Figure 7. (a,b) Thermogravimetric (TG) curves of polymer PBIP (a) and PBIP-Tb^{3+} complex (b).

Magnetic Property of PBIP-Tb^{3+} Complex

As mentioned in introduction, magnetism of polymeric complexes comes from the long range ordering of unpaired electrons through spin-spin interactions.[10] For PBIP, there is no unpaired electron, so it shows diamagnetism. After cleating with Tb^{3+}, electron transfers from MeBIP ligand to Tb^{3+} and unpaired electron appears in both Tb^{3+} and PBIP.[31] The long range ordering of unpaired electrons of Tb^{3+} and PBIP produces magnetism for PBIP-Tb^{3+} complex. The magnetic property of PBIP-Tb^{3+} complex was investigated as a function of temperature (T) and a function of magnetization (M). Figure 5 shows the temperature dependence of χT and the magnetic susceptibility (χ^{-1}) for PBIP-Tb^{3+} complex at an applied magnetic field of 30 kOe. The straight line is a fit to the Curie-Weiss law in the temperature range from 50 to 300 K. The room temperature χT product for PBIP-Tb^{3+} complex is 0.0113 emu/g/Oe·K ($T = 25\,^{\circ}C$). The χT *value* remains nearly constant down to 50 K and for lower temperature it decreases steeply to a value of 0.0046 emu/g/Oe·K at 5 K. The magnetic susceptibility for PBIP-Tb^{3+} complex conforms well to the Curie–Weiss law ($\chi = \frac{C}{T-\theta}$) in the range of 50–300 K. The results show that the Curie constant C is 0.012 and Curie–Weiss temperature θ is 2.6 K. Typical S shaped magnetic hysteresis loop (Figure 6) of PBIP-Tb^{3+} complex was measured at 5 K showing coercivity (H_c) of 22.1 Oe and remnant magnetization (M_r) of 0.038 emu/g. As a result of the little H_c[33] and S shaped hysteresis loop,[34] it can be concluded that PBIP-Tb^{3+} complex shows soft ferromagnetic property.

Thermal Property of PBIP and PBIP-Tb^{3+} Complex

Figure 7 illustrates the thermogravimetric (TG) curves of polymer PBIP and PBIP-Tb^{3+} complex. Both PBIP and PBIP-Tb^{3+} complex show good thermal property, because of the presence of benzimidazole ring and pyridine ring. For PBIP, the degradation temperature is about 370 °C for 5% weight loss. With temperature increasing from 370 °C to 450 °C, PBIP degrade quickly to 75% weight loss [Figure 7(a)]. Due to the loss of coordinated small molecules,[31] the initial degradation temperature of PBIP-Tb^{3+} complex is 250 °C, much lower than that of PBIP. The

degradation of PBIP-Tb^{3+} complex is a continuous weight loss process and the total weight loss is 38% from 250 °C to 700 °C, indicating that PBIP-Tb^{3+} complex does not decompose completely at 700 °C [Figure 7(b)]. Comparing to previously reported terbium polyaniline complex and terbium polythiophene complex,[35] the thermal stability of PBIP-Tb^{3+} is better.

CONCLUSIONS

In summary, homopolymer poly[6-(2,6-bis(1′-methylbenzimidazolyl)pyridin-4-yloxy)hexyl acrylate] (PBIP) and its terbium complex (PBIP-Tb^{3+}) were prepared. Fluorescence spectra confirm that MeBIP ligands of PBIP chelate with Tb^{3+} and UV–vis absorption spectra confirm the ratio of MeBIP and Tb^{3+} is 1:1 when forming complex. "S" shaped magnetic hysteresis loop and the low values of H_c and M_r indicate that PBIP-Tb^{3+} complex is soft ferromagnetic. In addition, TGA curves demonstrate that PBIP and PBIP-Tb^{3+} complex show good thermal stability.

ACKNOWLEDGMENTS

The authors are grateful for the financial support from National Science Foundation of China (Grant No. 21174129).

REFERENCES

1. Tong, S. Y.; Tung, M. J.; Ko, W. S.; Huang, Y. T.; Wang, Y. P.; Wang, L. C.; Wu, J. M. *J. Alloys Compd.* **2013**, *550*, 39.
2. Li, D.; Wang, Z.; Han, X. M.; Li, Y.; Guo, X. B.; Zuo, Y. L.; Xi, L. *J. Magn. Magn. Mater.* **2015**, *375*, 33.
3. Liu, Q.; Liu, X. X.; Shi, C. D.; Zhang, Y. P.; Feng, X. J.; Cheng, M.; Su, S.; Gu, J. D. *Dalton Trans.* **2015**, *44*, 19175.
4. Akhtar, N.; Polyakov, A. O.; Aqeel, A.; Gordiichuk, P.; Blake, G. R.; Baas, J.; Amenitsch, H.; Herrmann, A.; Rudolf, P.; Palstra, T. T. M. *Small* **2014**, *10*, 4912.
5. Luo, J.; Wang, Y. H.; Ren, R.; Sun, W. L.; Shen, Z. Q. *Polym. Adv. Technol.* **2015**, *26*, 432.
6. Zhou, X.; Sun, W. L.; Shen, Z. Q. *Acta Polym. Sin.* **2014**, 1251.
7. Luo, J.; Wang, Y. H.; Ren, R.; Sun, W. L.; Shen, Z. Q. *J. Appl. Polym. Sci.* **2014**, *131*, DOI: 10.1002/app.46081.
8. Ding, N. W.; Sun, W. L.; Lin, Y.; Shen, Z. Q. *Chin. J. Polym. Sci.* **2012**, *30*, 759.
9. Zheng, R. H.; Jiang, H. J.; Guo, H. C.; Sun, W. L. *Acta Polym. Sin.* **2011**, 435.
10. Wang, Y. H.; Luo, J.; Ren, R.; Sun, W. l.; Shen, Z. Q. *Polym. Sci. Eng.* **2014**, *30*, 2014.
11. Wu, Y.; Hu, J.; Zhang, C.; Han, J.; Wang, Y.; Kumar, B. *J. Mater. Chem. A* **2015**, *3*, 97.
12. Michal, B. T.; McKenzie, B. M.; Felder, S. E.; Rowan, S. J. *Macromolecules* **2015**, *48*, 3239.
13. Wang, Z. H.; Fan, W. R.; Tong, R.; Lu, X. L.; Xia, H. S. *RSC Adv.* **2014**, *4*, 25486.
14. Lai, H. Q.; Zhao, Z. N.; Li, L. L.; Zheng, W. J.; Chen, T. F. *Metallomics* **2015**, *7*, 439.
15. Zhao, Z. N.; Luo, Z. D.; Wu, Q.; Zheng, W. J.; Feng, Y. X.; Chen, T. F. *Dalton Trans.* **2014**, *43*, 17017.
16. Elagab, H. A.; Alt, H. G. *Eur. Polym. J.* **2015**, *71*, 85.
17. Chao, S. J.; Bai, Z. Y.; Cui, Q.; Yan, H. Y.; Wang, K.; Yang, L. *Carbon* **2015**, *82*, 77.
18. Saikia, E.; Borpuzari, M. P.; Chetia, B.; Kar, R. *Spectrochim. Acta Part A* **2016**, *152*, 101.
19. Li, Z. Q.; Hou, Z. H.; Ha, D. H.; Li, H. R. *Asian J. Chem.* **2015**, *10*, 2720.
20. Chetia, B.; Iyer, P. K. *Sens. Actuators, B* **2014**, *201*, 191.
21. Nagashima, T.; Nakabayashi, T.; Suzuki, T.; Kanaizuka, K.; Ozawa, H.; Zhong, Y. W.; Masaoka, S.; Sakai, K.; Haga, M. *Organometallics* **2014**, *33*, 4893.
22. Yang, W. W.; Zhong, Y. W. *Chin. J. Chem.* **2013**, *31*, 329.
23. Yang, Y.; Bai, F. Q.; Zhang, H. X.; Zhou, X.; Sun, C. C. *Comput. Theor. Chem.* **2011**, *963*, 298.
24. Zhang, D. P.; Zhuo, S. P.; Zhang, H. Y.; Wang, P.; Jiang, J. Z. *Dalton Trans.* **2015**, *44*, 4655.
25. Jeon, L. R.; Calancea, S.; Panja, A.; Pinero Cruz, D. M.; Koumousi, E. S.; Dechambenoit, P.; Coulon, C.; Wattiaux, A.; Rosa, P.; Mathoniere, C.; Clerac, R. *Chem. Sci.* **2013**, *4*, 2463.
26. Panja, A.; Guionneau, P.; Jeon, L. R.; Holmes, S. M; Clerac, R.; Mathoniere, C. *Inorg. Chem.* **2012**, *51*, 12350.
27. Qian, J.; Hu, J. C.; Yoshikawa, H.; Zhang, J. F.; Awaga, K.; Zhang, C. *Eur. J. Inorg. Chem.* **2015**, *2015*, 2110.
28. Nihei, M.; Okamoto, Y.; Sekine, Y.; Hoshino, N.; Shiga, T.; Liu, I. P. C.; Oshio, H. *Angew. Chem.* **2012**, *51*, 6361.
29. Chong, Y. K.; Moad, G.; Rizzardo, E.; Thang, S. H. *Macromolecules* **2007**, *40*, 4446.
30. Jackson, A. C.; Beyer, F. L.; Price, S. C.; Rinderspacher, B. C.; Lambeth, R. H. *Macromolecules* **2013**, *46*, 5416.
31. Piguet, C.; Williams, A. F.; Bernardiuelli, G.; Moret, E.; Biinzli, J. C. *Helv. Chim. Acta* **1992**, *75*, 1697.
32. Chen, Y.; Xing, Z.; Cao, S.; Wang, Y. *J. Rare Earth* **2016**, *34*, 240.
33. Wu, L. B.; Lv, Z. Q.; Chen, Q.; Chen, L. M.; Jiang, J. X. *Chem. J. Chinese U* **2014**, *32*, 1744.
34. Zhong, M.; Li, Y.; Tariq, M.; Hu, Y.; Li, W.; Zhu, M.; Jin, H.; Li, Y. *J. Alloy. Compd.* **2016**, *675*, 286.
35. Rafiqi, F. A.; Majid, K. *Synth. Met.* **2015**, *202*, 147.